

# Decoherence of tripartite states - a trapped ion coupled to an optical cavity

S. Shelly Sharma\* and E. de Almeida†

*Depto. de Física, Universidade Estadual de Londrina, Londrina 86051-990, PR Brazil*

N. K. Sharma‡

*Depto. de Matemática, Universidade Estadual de Londrina, Londrina 86051-990 PR, Brazil*

Corresponding author: S. Shelly Sharma (shelly@uel.br)

We investigate the decoherence process of three qubit system obtained by manipulating the state of a trapped two-level ion coupled to an optical cavity. Interaction of the ion with a resonant laser and the cavity field tuned to red sideband of ionic vibrational motion, generates tripartite entanglement of internal state of the ion, vibrational state of ionic center of mass motion and the cavity field state. Non-dissipative decoherence occurs due to entanglement of the system with the environment, modeled as a set of noninteracting harmonic oscillators. Analytic expressions for the state operator of tripartite composite system, the probability of generating maximally entangled GHZ state, and the population inversion have been obtained. Coupling to environment results in exponential decay of off diagonal matrix elements of the state operator with time as well as a phase decoherence of the component states.

Numerical calculations to examine the time evolution of GHZ state generation probability and population inversion for different values of system environment coupling strengths are performed. Using negativity as an entanglement measure and linear entropy as a measure of mixedness, the entanglement dynamics of the tripartite system in the presence of decoherence sources has been analyzed. The maximum tripartite entanglement is found to decrease with increase in the strength of system-environment coupling. The negativity as well as the linear entropy as entanglement measures give qualitatively similar results, uniquely identifying maximally entangled and separable states of the system. For large values of system-environment coupling strength, the mixed states of the composite system lying at the boundary of entangled-separable region are reached. For these states the negativity and linear entropy show distinctly different behaviour. This can be understood by noting that whereas the negativity measures entanglement generating quantum correlations, the linear entropy measures all correlations that reduce the purity of the state.

**Keywords:** Trapped ions, Cavity QED, Tripartite entanglement, GHZ state generation, Non-Dissipative Decoherence, Negativity, Linear entropy, Mixed states

## INTRODUCTION

Controlled manipulation of quantum states and implementation of quantum logic gates are essential elements of a quantum computer. Quantum computation relies on nonclassical properties of qubits such as entanglement. Entanglement dynamics is of utmost importance to quantum communication [1], dense coding [2] and quantum teleportation [3], as well. Cold ions in a linear trap [4] offer a promising physical system to implement quantum computation, as each ion allows two qubit state manipulation. One of the experimental efforts to realize multipartite entanglement involves trapping two level ion in an optical cavity. Coupling of trapped ion to quantized field inside an optical cavity has been successfully achieved [5]. More than one trapped ions can be used to construct a more complex multiple function system in which quantum states of several trapped ions entangled with cavity photons are manipulated in a controlled manner. A string of trapped ions in a cavity may be used for implementing quantum gates [6]. In quantum networks involving cavity QED setups [7], quantum information is stored and processed by ions trapped in a cavity. De-coherence of quantum systems is one of the major hurdles to implement quantum computers. Suppression of quantum coherence occurs due to interactions of the quantum system with environment resulting in random and unknown perturbations of system Hamiltonian. In a previous article [8], we proposed a scheme to generate three qubit maximally entangled GHZ state, using trapped ion interacting with a resonant external laser and sideband tuned single mode of a cavity field. In this article, we investigate the decoherence process of three qubit system obtained by manipulating the state of a two level trapped ion coupled to an optical cavity. In the context of a qubit based on a single  $\text{Ca}^+$  ion, Schmidt-Kaler et al [9] have found magnetic field fluctuations and laser frequency fluctuations to be the major decoherence sources. Decoherence of motional quantum states of a trapped atom coupled to engineered phase and amplitude reservoirs has been measured [10, 11]. The trap frequency was changed by applying potentials to trap electrodes to simulate a phase reservoir. In general the environment or heat bath is modeled as a system of noninteraction boson modes [12]. It is known that for harmonic systems a heat bath is effectively equivalent

to an external uncorrelated random force acting on the quantum system. As such the decoherence effects due to magnetic field fluctuations, laser frequency fluctuations, and potentials applied to electrodes can be modeled as a system of noninteracting boson modes. Other important decoherence sources are cavity losses and spontaneous decay. The case where spontaneous decay effects and cavity losses become important has been examined by Fidio et al. [13]. In the present work, these two effects are assumed to be negligible.

As the laser-ion interaction times involved in experiments with ions trapped in a cavity are in the micro seconds range, Markovian approximation is likely to yield undesirable results. We consider here only adiabatic decoherence of the system with no energy exchange between the quantum system and environment. A detailed discussion on adiabatic decoherence has been given by Mozyrsky and Privman in ref. [14]. Starting from an initial state in which the system and environment are in a separable state, the state operator of the ion-cavity system is obtained by tracing over the environment degrees of freedom. Coherent states are used to evaluate the trace [14]. The decoherence effects result in a state operator with off diagonal matrix elements decaying with time, in the eigen basis of the interaction Hamiltonian. The state operator is used to examine the decoherence effects on the probability of generating maximally entangled tripartite GHZ state and population inversion of two level ion. As the coherences decrease the system tends to a purely mixed state of energy eigenvectors. Decoherence of tripartite entanglement is analyzed by applying the Peres-Horodecki condition for separability [15] to bipartite decompositions of the composite system. A state is separable if the partial transpose of its density matrix with respect to a subsystem is positive semidefinite. An entangled state violates the positive partial transpose (PPT) separability criterion. Negativity [16] is an entanglement measure based on (PPT) separability criterion. We use Negativity to characterize the entanglement and linear entropy to measure the mixedness of three subsystems.

### UNITARY EVOLUTION OF ISOLATED SYSTEM

Consider a single two-level ion trapped in a high finesse optical cavity. The frequency of radio frequency (Paul) trap along  $x$  axis is  $\nu$  and the excitation energy of the ion is  $\hbar\omega_0$ . The ion is radiated by an external resonant laser of frequency  $\omega_L$  and interacts with the single mode cavity field of frequency  $\omega_c$  tuned to red sideband of ionic vibrational motion. Interaction with external laser field as well as the cavity field generates entanglement of internal states of the ion, vibrational states of ionic center of mass, and the cavity field number state. The free Hamiltonian of the system is

$$\hat{H}_{0S} = \hbar\nu \left( \hat{a}^\dagger \hat{a} + \frac{1}{2} \right) + \hbar\omega_c \hat{b}^\dagger \hat{b} + \frac{\hbar\omega_0}{2} \hat{\sigma}_z \quad , \quad (1)$$

$\hat{a}^\dagger(\hat{a})$  and  $\hat{b}^\dagger(\hat{b})$  being the creation(destruction) operators for vibrational phonon and cavity field photon respectively. With the ion placed close to the node of cavity field standing wave, the interaction Hamiltonian is given by

$$\begin{aligned} \hat{H}_I = & \hbar\Omega[\hat{\sigma}_+ \exp[i\eta_L(\hat{a} + \hat{a}^\dagger) - i\omega_L t] + \hat{\sigma}_- \exp[i\eta_L(\hat{a} + \hat{a}^\dagger) + i\omega_L t]] \\ & + \hbar g (\hat{\sigma}_+ \hat{b} + \hat{\sigma}_- \hat{b}^\dagger) \sin[\eta_c(\hat{a} + \hat{a}^\dagger)] \quad , \end{aligned} \quad (2)$$

where  $\Omega$ ,  $g$ ,  $\eta_L$ ,  $\eta_c$  are the Rabi frequency, the ion-cavity coupling strength, ion-laser Lamb Dicke parameter, and ion-cavity field Lamb Dicke parameter, respectively. We work in the Lamb Dicke regime that is  $\eta_L \ll 1$ ,  $\eta_c \ll 1$ . In the interaction picture determined by the transformation  $\hat{U} = \exp(i\hat{H}_{0S}t/\hbar)$  and rotating wave approximation, for  $\omega_L = \omega_0$  and  $\omega_c = \omega_0 - \nu$ , the interaction Hamiltonian reduces to

$$\hat{H}_{II} = \hbar\Omega[\hat{\sigma}_+ + \hat{\sigma}_-] + \hbar g \eta_c [\hat{\sigma}_+ \hat{b} \hat{a} + \hat{\sigma}_- \hat{b}^\dagger \hat{a}^\dagger] \quad . \quad (3)$$

The unitary evolution of the isolated system in interaction picture is given by

$$i\hbar \frac{\partial \Psi_I(t)}{\partial t} = \hat{H}_{II} \Psi_I(t),$$

where  $\Psi_I(t) = \exp(i\hat{H}_{0S}t/\hbar)\Psi_S(t)$ .

### Basis truncation

We expand  $\hat{H}_{II}$  in the space of basis vectors  $|i, k, l\rangle$  as

$$\hat{H}_{II} = \sum_{i,k,l,i',k',l'} \langle i', k', l' | \hat{H}_{II} | i, k, l \rangle | i', k', l' \rangle \langle i, k, l |, \quad (4)$$

where  $i = (g \text{ or } e)$  and  $k, l(0, 1, \dots, \infty)$ , denote the state of ionic vibrational motion and the cavity field number state, respectively. We isolate a four dimensional vector space containing the computational basis vectors  $|g, m-1, n-1\rangle, |e, m-1, n-1\rangle, |g, m, n\rangle$  and  $|e, m, n\rangle$  for a given choice of  $m, n$  values. The matrix representing the interaction Hamiltonian acting in four dimensional space is

$$\hat{H}_{IS} \rightarrow \begin{bmatrix} 0 & \hbar\Omega & 0 & 0 \\ \hbar\Omega & 0 & \hbar g\eta_c \sqrt{mn} & 0 \\ 0 & \hbar g\eta_c \sqrt{mn} & 0 & \hbar\Omega \\ 0 & 0 & \hbar\Omega & 0 \end{bmatrix}. \quad (5)$$

The unitary transformation that diagonalizes  $\hat{H}_{IS}$  is easily obtained and yields the eigenvectors satisfying  $\hat{H}_{IS}\Phi_p = E_p\Phi_p$ , ( $p = 1, 4$ ). The computational basis vectors are related to the eigenvectors  $\Phi_p$  through

$$\begin{bmatrix} |g, m-1, n-1\rangle \\ |e, m-1, n-1\rangle \\ |g, m, n\rangle \\ |e, m, n\rangle \end{bmatrix} = \begin{bmatrix} \frac{A+B}{\sqrt{2}} & \frac{A-B}{\sqrt{2}} & \frac{A-B}{\sqrt{2}} & \frac{-A-B}{\sqrt{2}} \\ \frac{A-B}{\sqrt{2}} & \frac{-A-B}{\sqrt{2}} & \frac{A+B}{\sqrt{2}} & \frac{A-B}{\sqrt{2}} \\ \frac{B-A}{\sqrt{2}} & \frac{A+B}{\sqrt{2}} & \frac{A+B}{\sqrt{2}} & \frac{A-B}{\sqrt{2}} \\ \frac{-A-B}{\sqrt{2}} & \frac{B-A}{\sqrt{2}} & \frac{A-B}{\sqrt{2}} & \frac{-A-B}{\sqrt{2}} \end{bmatrix} \begin{bmatrix} \Phi_1 \\ \Phi_2 \\ \Phi_3 \\ \Phi_4 \end{bmatrix}, \quad (6)$$

where  $a_{mn} = \frac{1}{2}g\eta_c\sqrt{mn}$ ,  $\mu_{mn} = \sqrt{a_{mn}^2 + \Omega^2}$ ,  $A^2 = (\mu_{mn} + \Omega)/4\mu_{mn}$ , and  $B^2 = (\mu_{mn} - \Omega)/4\mu_{mn}$ . The corresponding eigenvalues are  $E_1 = \hbar(\mu_{mn} - a_{mn})$ ,  $E_2 = -\hbar(\mu_{mn} + a_{mn})$ ,  $E_3 = \hbar(\mu_{mn} + a_{mn})$ , and  $E_4 = \hbar(a_{mn} - \mu_{mn})$ .

### Unitary evolution in truncated basis space

Unitary time evolution of the system due to interaction operator  $\hat{H}_{IS}$  had been obtained, analytically, in ref. [8] for initial states  $|g, m-1, n-1\rangle$ , and  $|e, m-1, n-1\rangle$ . For interaction time  $t_p$  such that  $\mu_{mn}t_p = p\pi$ ,  $p = 1, 2, \dots$ , the initial state  $|g, m-1, n-1\rangle$  is found to evolve into

$$\Psi_I(t_p) = (-1)^p [\cos(a_{mn}t_p) |g, m-1, n-1\rangle - i \sin(a_{mn}t_p) |e, m, n\rangle], \quad (7)$$

Now consider a special initial state with the ion in its ground state occupying the lowest energy trap state, while the cavity is prepared in vacuum state ( $m = n = 1$ ). Without taking into consideration the decoherence effects, the ratio  $\alpha = (\mu_{11}/a_{11})$  determines the interaction time  $t_p$  needed to generate maximally entangled tripartite GHZ state. Leaving out an overall phase factor, for an interaction time  $t_p$  such that  $a_{11}t_p = \frac{\pi}{4}, \frac{5\pi}{4}, \dots$ , ( $\alpha = 4$ ), the system is found to be in the state

$$\Psi_{GHZ,I}^-(t_p) = \frac{1}{\sqrt{2}} (|g, 0, 0\rangle - i |e, 1, 1\rangle), \quad (8)$$

and for  $a_{11}t_p = \frac{3\pi}{4}, \frac{7\pi}{4}, \dots$ , the state of the system is

$$\Psi_{GHZ,I}^+(t_p) = \frac{1}{\sqrt{2}} (|g, 0, 0\rangle + i |e, 1, 1\rangle). \quad (9)$$

The density operator representation for these states is

$$\hat{\rho}_{GHZ,I}(t_p) = |\Psi_{GHZ,I}(t_p)\rangle \langle \Psi_{GHZ,I}(t_p)|. \quad (10)$$

Neglecting an overall phase factor, the states can be written in Schrodinger picture as

$$\begin{aligned} \Psi_{GHZ,I}^-(t_p) &= \frac{1}{\sqrt{2}} (|g, 0, 0\rangle - i \exp(-i2\omega_0 t) |e, 1, 1\rangle) \\ \Psi_{GHZ,I}^+(t_p) &= \frac{1}{\sqrt{2}} (|g, 0, 0\rangle + i \exp(-i2\omega_0 t) |e, 1, 1\rangle). \end{aligned}$$

**DECOHERENCE OF UNITARY EVOLUTION IN TRUNCATED SPACE**

We notice that the interaction Hamiltonian  $\hat{H}_{II}$  (Eq. (4)) connects the model space states to states outside the model space. For the specific case of initial state  $|g, 0, 0\rangle$ , the leading term in the probability of finding a state outside the model space varies as  $t^8$ . The states outside the model space may be considered as part of the environment states. The resulting decoherence effects can be accounted for by coupling the model space interaction Hamiltonian to the environment modeled as a set of oscillators. We recall that the scattering outside the model space results in internal states linked to motional states with phonon number  $> 1$ , resulting in heating of the ions. In a realistic experimental set-up, the heating of ions trapped in a radio-frequency trap occurs due to the electric field noise from the trap electrodes [17]. The two effects can not be separated. Error in initial phonon state preparation can also add to decoherence by additional scattering to states outside the model space. The cavity states with number of photons  $> 1$ , are created and annihilated in the vector space outside the model space. In a lossy cavity photons leaving the cavity are akin to state reduction which can contribute to creating states in the model space. In this work we consider the average decoherence effects arising due to the decoherence sources such as magnetic field fluctuations, laser frequency fluctuations, potentials applied to electrodes and coupling to states outside the model space. The random perturbations of the Hamiltonian are accounted for by coupling the model space interaction Hamiltonian to environment modeled as a set of non-interacting harmonic oscillators [12]. The phase decoherence results in decay of entanglement needed for various computation related tasks. In interaction picture the Hamiltonian for the system and environment, with  $\hat{H}_{IS}$  coupled to environment is given by

$$\hat{H} = \hat{H}_{IS} + \sum_k \hbar\omega_k \hat{B}_k^\dagger \hat{B}_k + \hat{H}_{IS} \sum_k \left( g_k^* \hat{B}_k + g_k \hat{B}_k^\dagger \right), \quad (11)$$

where  $\hat{B}_k^\dagger$  and  $\hat{B}_k$  are bosonic creation and destruction operators for the environment mode of frequency  $\omega_k$ . The coefficients  $g_k, g_k^*$  are the system environment couplings.

The initial state of the system is assumed to be  $\hat{\rho}_S(0)$ , while the environment is in an uncorrelated state,  $\prod_k \hat{\theta}_k$ , where  $\hat{\theta}_k = Z_k^{-1} e^{-\beta\omega_k \hat{B}_k^\dagger \hat{B}_k}$  and  $Z_k = (1 - e^{-\beta\omega_k})^{-1}$ . The assumption that the environment is in an uncorrelated state allows exact solvability, though no physical fundamental reason can be given for this. However, as the initial state of the system is a doctored state, the assumption of separability of system environment state at  $t = 0$ , holds. The state operator for the system is obtained by solving

$$\hat{\rho}_{IS}(t) = Tr_E \left( e^{-\frac{i\hat{H}t}{\hbar}} \hat{\rho}_S(0) \prod_k \hat{\theta}_k e^{\frac{i\hat{H}t}{\hbar}} \right), \quad (12)$$

where  $Tr_E$  refers to the operation of tracing over bosonic degrees of freedom used to model the environment. Working in the eigen basis of  $\hat{H}_{IS}$ , we may write

$$\begin{aligned} \hat{\rho}_{IS}(t) = & \sum_{i,j} Tr_E \left( e^{-it \sum_k (\omega_k \hat{B}_k^\dagger \hat{B}_k + \frac{E_i}{\hbar} (g_k^* \hat{B}_k + g_k \hat{B}_k^\dagger))} \prod_k \hat{\theta}_k e^{it \sum_k (\omega_k \hat{B}_k^\dagger \hat{B}_k + \frac{E_j}{\hbar} (g_k^* \hat{B}_k + g_k \hat{B}_k^\dagger))} \right) \\ & \exp \left[ \frac{-i(E_i - E_j)t}{\hbar} \right] \langle \Phi_i | \hat{\rho}_S(0) | \Phi_j \rangle | \Phi_i \rangle \langle \Phi_j |. \end{aligned} \quad (13)$$

The trace over bosonic bath states is evaluated by using coherent states [14] and the resulting state operator for the system is

$$\begin{aligned} \hat{\rho}_{IS}(t) = & \sum_{i,j} \langle \Phi_i | \hat{\rho}_S(0) | \Phi_j \rangle \exp \left( \frac{-(E_i - E_j)^2 \Gamma(t)}{4.0 \hbar^2} \right) \\ & \exp \left[ -i \left( \frac{(E_i - E_j)t}{\hbar} + \frac{(E_i^2 - E_j^2)C(t)}{\hbar^2} \right) \right] | \Phi_i \rangle \langle \Phi_j |, \end{aligned} \quad (14)$$

where, using the notation of ref. [14],

$$\Gamma(t) = 8 \sum_k \frac{|g_k|^2}{\omega_k^2} \sin^2 \left( \frac{\omega_k t}{2} \right) \coth \left( \frac{\beta\omega_k}{2} \right), \quad (15)$$

and

$$C(t) = \sum_k \frac{|g_k|^2}{\omega_k^2} (\sin(\omega_k t) - \omega_k t). \quad (16)$$

The summation over bath modes in Eqs. (15) and (16) can be replaced by integration over frequency by introducing a frequency dependent density function. For an ohmic dissipation characterized by density function  $D(\omega) |g|^2 = \kappa \omega \exp(-\omega/\omega_c)$ , we obtain

$$\Gamma(t) = 8\kappa \int d\omega \frac{\exp(-\omega/\omega_c)}{\omega} \coth\left(\frac{\beta\omega}{2}\right) \sin^2\left(\frac{\omega t}{2}\right), \quad (17)$$

and

$$C(t) = \kappa \int d\omega \frac{\exp(-\omega/\omega_c)}{\omega} (\sin(\omega t) - \omega t), \quad (18)$$

where  $\omega_c$  is a cut off frequency and constant  $\kappa$  a measure of system-bath coupling strength.

$$\textbf{Initial State } \hat{\rho}_S(0) = |g, m-1, n-1\rangle \langle g, m-1, n-1|$$

We consider the case when the system is prepared, at  $t = 0$ , in the state  $\hat{\rho}_S(0) = |g, m-1, n-1\rangle \langle g, m-1, n-1|$ . The state operator  $\hat{\rho}_{IS}(t)$  obtained by putting in the energy spectrum of  $\hat{H}_{IS}$  in Eq. (14) is

$$\begin{aligned} \hat{\rho}_{IS}(t) = & \frac{(A+B)^2}{2} [|\Phi_1\rangle \langle \Phi_1| + |\Phi_4\rangle \langle \Phi_4|] \\ & + \frac{(A-B)^2}{2} (|\Phi_2\rangle \langle \Phi_2| + |\Phi_3\rangle \langle \Phi_3|) \\ & - \frac{(A+B)^2}{2} \exp\left(-(\mu_{mn} - a_{mn})^2 \Gamma(t)\right) \\ & \times [\exp(-i2(\mu_{mn} - a_{mn})t) |\Phi_1\rangle \langle \Phi_4| + \exp(i2(\mu_{mn} - a_{mn})t) |\Phi_4\rangle \langle \Phi_1|] \\ & + \frac{(A-B)^2}{2} \exp\left(-(\mu_{mn} + a_{mn})^2 \Gamma(t)\right) \\ & \times [\exp(i2(\mu_{mn} + a_{mn})t) |\Phi_2\rangle \langle \Phi_3| + \exp(-i2(\mu_{mn} + a_{mn})t) |\Phi_3\rangle \langle \Phi_2|] \\ & + \frac{(A^2 - B^2)}{2} \exp(-\mu_{mn}^2 \Gamma(t)) \\ & \times [\exp[-i(2\mu_{mn}t - \varphi(t))] |\Phi_1\rangle \langle \Phi_2| + \exp[i(2\mu_{mn}t - \varphi(t))] |\Phi_2\rangle \langle \Phi_1| \\ & - \exp[-i(2\mu_{mn}t + \varphi(t))] |\Phi_3\rangle \langle \Phi_4| - \exp[i(2\mu_{mn}t + \varphi(t))] |\Phi_4\rangle \langle \Phi_3|] \\ & + \frac{(A^2 - B^2)}{2} \exp(-a_{mn}^2 \Gamma(t)) \\ & \times [\exp[i(2a_{mn}t + \varphi(t))] |\Phi_1\rangle \langle \Phi_3| + \exp[-i(2a_{mn}t + \varphi(t))] |\Phi_3\rangle \langle \Phi_1| \\ & - \exp[i(2a_{mn}t - \varphi(t))] |\Phi_2\rangle \langle \Phi_4| - \exp[-i(2a_{mn}t - \varphi(t))] |\Phi_4\rangle \langle \Phi_2|], \end{aligned} \quad (19)$$

where  $\varphi(t) = 4\mu_{mn}a_{mn}C(t)$ . The state operator  $\hat{\rho}_{IS}(t)$  contains information about the decay of coherences due to coupling of the system with the environment.

## DECOHERENCE AND GHZ STATE GENERATION PROBABILITY

Undergoing decoherence free time evolution, for  $\hat{\rho}_S(0) = |g, 0, 0\rangle \langle g, 0, 0|$  and the interaction time  $t_p$  such that  $a_{11}t_p = \frac{\pi}{4}, \mu_{11}t_p = \pi$  ( $\alpha = 4$ ), the system evolves into a maximally entangled tripartite two mode GHZ state given by Eq. (8). We define GHZ state generation probability as  $P_{GHZ}(t) = \text{tr}\left(\hat{\rho}_{IS}(t)\hat{\rho}_{GHZ,I}^{(-)}\right)$ , where  $\hat{\rho}_{GHZ,I}^{(-)} = |\Psi_{GHZ,I}^-\rangle \langle \Psi_{GHZ,I}^-|$ . Using Eq. (19) we write down the density operator  $\hat{\rho}_{IS}(t)$  for the choice  $m = 1, n = 1$  and

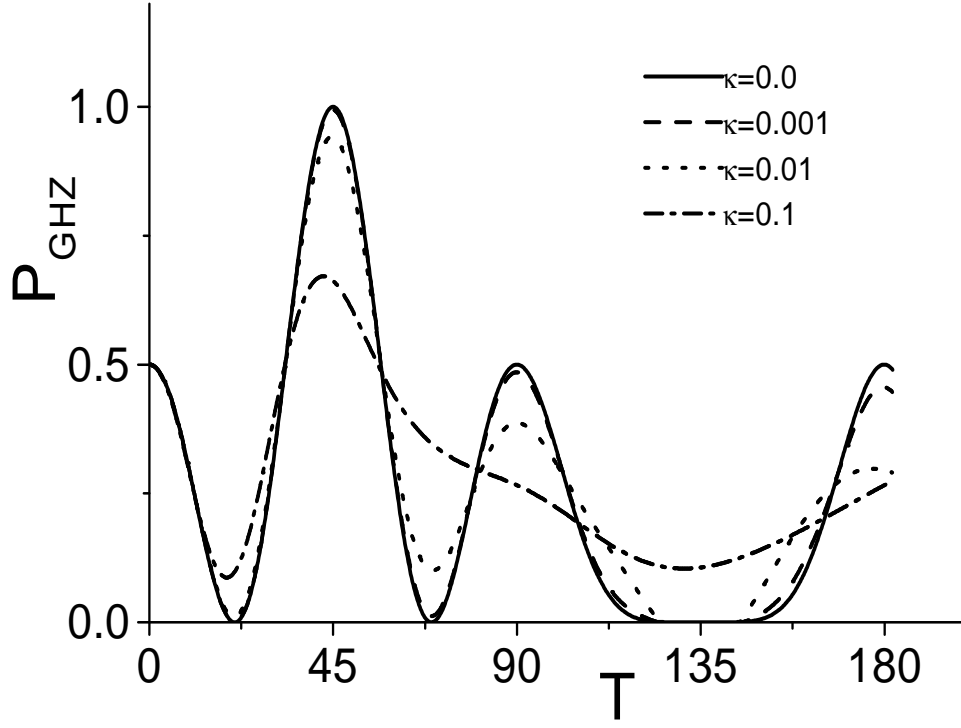


FIG. 1:  $P_{GHZ}(t)$  as a function of scaled time variable  $T(= a_{11}t)$ , for the choice  $\mu_{11} \setminus a_{11} = 4$ , and  $\kappa = 0, 0.001, 0.01$  and  $0.1$ .

evaluate  $P_{GHZ}(t)$ . The resulting expression for GHZ state generation probability is

$$\begin{aligned}
P_{GHZ}(t) = & \frac{1}{2} + \frac{\Omega^2}{4\mu_{11}^2} \left( \exp\left(\frac{-\mu_{11}^2 \Gamma(t)}{4.0}\right) \cos(2\mu_{11}t) \cos(\varphi(t)) \right) \\
& + \frac{\Omega^2}{4\mu_{11}^2} \left( \exp\left(\frac{-a_{11}^2 \Gamma(t)}{4.0}\right) \sin(2a_{11}t) \cos(\varphi(t)) - 1 \right) \\
& + \frac{1}{2} \left( \frac{\mu_{11} - a_{11}}{2\mu_{11}} \right)^2 \exp\left(\frac{-(\mu_{11} - a_{11})^2 \Gamma(t)}{4.0}\right) \sin[2(\mu_{11} - a_{11})t] \\
& - \frac{1}{2} \left( \frac{\mu_{11} + a_{11}}{2\mu_{11}} \right)^2 \exp\left(\frac{-(\mu_{11} + a_{11})^2 \Gamma(t)}{4.0}\right) \sin[2(\mu_{11} + a_{11})t]. \tag{20}
\end{aligned}$$

We also calculate the population inversion defined as  $I = P_g - P_e$ , where  $P_g(P_e)$  is the probability of finding the ion in ground (excited) state. For the choice  $m = 1, n = 1$ , in the state  $\hat{\rho}_{IS}(t)$  of Eq. (19), we get

$$\begin{aligned}
I = & \frac{\mu_{11} + a_{11}}{2\mu_{11}} \left( \exp\left(-(\mu_{11} - a_{11})^2 \Gamma(t)\right) \cos[2(\mu_{11} - a_{11})t] \right) \\
& + \frac{\mu_{11} + a_{11}}{2\mu_{11}} \left( \exp\left(-(\mu_{11} + a_{11})^2 \Gamma(t)\right) \cos[2(\mu_{11} + a_{11})t] \right). \tag{21}
\end{aligned}$$

In the limit  $\kappa \rightarrow 0$  the Eqs. (19), (20) and (21) reduce to decoherence free evolution of the state operator, the GHZ state generation probability, and the population inversion, respectively. As the cavity is initially in vacuum state and ionic center of mass in the lowest energy trap state, decoherence effects due to cavity decay and heating are expected to be small and have not been considered.

### NEGATIVITY AND LINEAR ENTROPY

The state of three qubit composite system is represented by  $\hat{\rho}_{IS}(t) = \hat{\rho}_{ABC}(t)$ , where  $A, B$ , and  $C$  refer to the internal state of two-level ion, the state of vibrational motion, and the cavity state respectively. A pure state of a

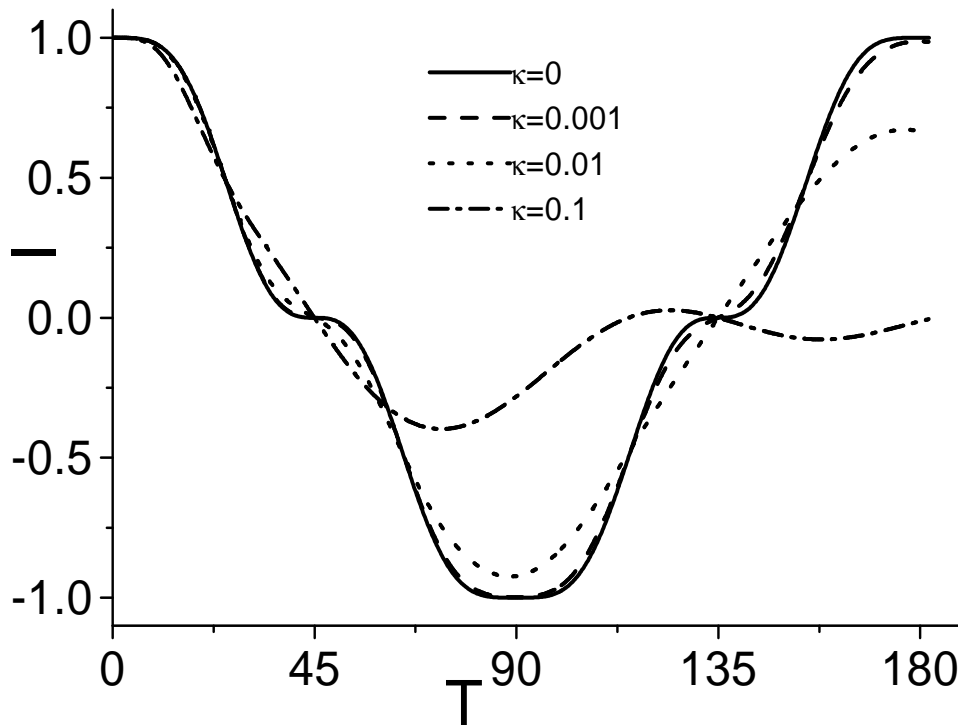


FIG. 2: Population inversion  $I(t)$ , as a function of scaled time variable  $T(= a_{11}t)$ , for the choice  $\mu_{11} \setminus a_{11} = 4$ , and  $\kappa = 0, 0.001, 0.01$  and  $0.1$ .

tripartite system can be separable, or entangled. Entangled state may or may not have(biseparable) true tripartite entanglement. Bipartite entanglement is relatively well understood. Entanglement content of a tripartite system may be measured through the entanglement of its bipartite decompositions that is  $A+(BC)$ ,  $B+(AC)$ , and  $C+(AB)$ . The decoherence effects result in a composite state  $\hat{\rho}_{ABC}(t)$ , which is usually a mixed state. Mixed state entanglement is less understood than the pure state entanglement. On examining Eq. (19), in which the state operator is expressed in the eigen-basis of  $\hat{H}_{IS}$ , we notice that the diagonal matrix elements of density matrix are not affected by coupling to the environment, whereas the moduli of off diagonal matrix elements decay with time. Consequently, when only non-dissipative decoherence is present the trace of  $\hat{\rho}_{ABC}(t)$  remains constant with time and the eigenvalues continue to be positive. Since  $\hat{\rho}_{ABC}(t)$  is positive definite, we use negativity proposed by Vidal and Werner [16] as an entanglement measure for pure as well as mixed states. Negativity is based on partial transpose of density matrix of composite system with respect to a subsystem.

The state of a bipartite system, composed of subsystems  $A$  and  $B$  in finite dimensional Hilbert spaces  $d_A$  and  $d_B$ , is written as

$$\hat{\rho} = \sum_{i,j=1}^{d_A} \sum_{m,r=1}^{d_B} \langle i, m | \hat{\rho} | j, r \rangle | i, m \rangle \langle j, r |. \quad (22)$$

The partial transpose of density operator with respect to sub-system  $A$  is defined as

$$\hat{\rho}^{TA} = \sum_{i,j=1}^{d_A} \sum_{m,r}^{d_B} \langle i, m | \hat{\rho} | j, r \rangle | j, m \rangle \langle i, r |. \quad (23)$$

The partial transpose of density matrix of an entangled state is not positive definite. Negativity defined as  $N^A = \sum_i |\lambda_i|$ , where  $\lambda_i$  are the negative eigenvalues of  $\hat{\rho}^{TA}$  is a measure of entanglement of quantum system  $A$  with  $B$ . For a separable state  $N^A = 0$  and at maximal entanglement value of  $N^A$  depends on dimension  $d_A$ . For the tripartite system at hand, we construct the partial transpose with respect to sub-systems  $A$ ,  $B$  or  $C$ , while keeping the composite state of the remaining two sub-systems unaltered. For the density matrix operator  $\hat{\rho}_{ABC}(t)$  acting on

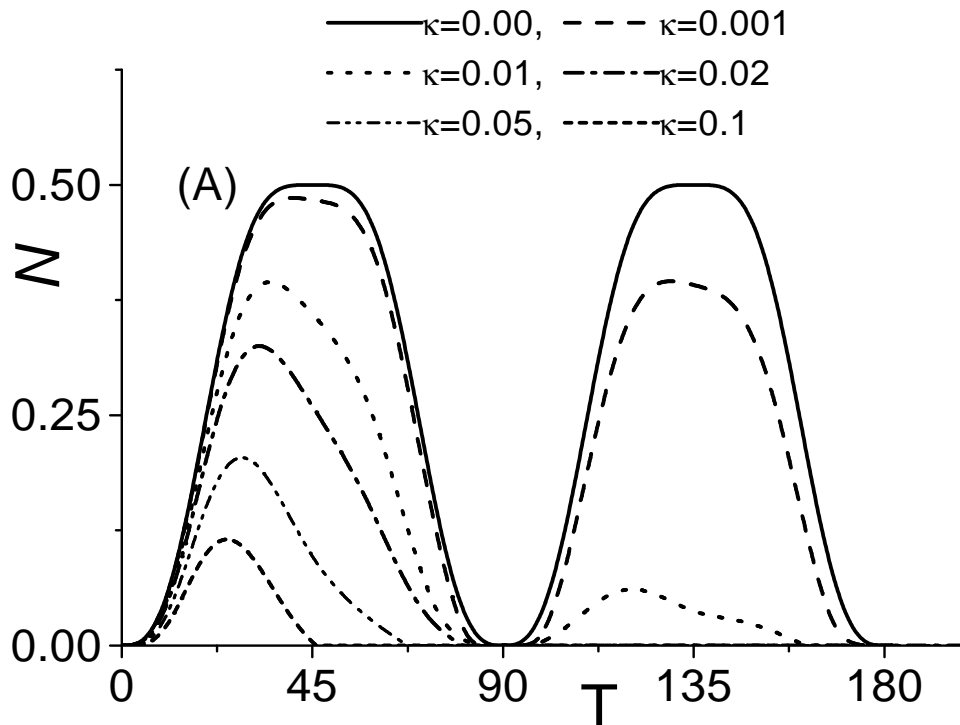


FIG. 3:  $N$ , calculated from  $\hat{\rho}^{TA}$ , as a function of scaled time variable  $T(= a_{11}t)$ , for the choice  $\mu_{11}/a_{11} = 4$ , and  $\kappa = 0, 0.001, 0.01, 0.02, 0.05$  and  $0.1$ .

composite space, the transpose with respect to sub-system A reads as

$$\hat{\rho}^{TA} = \sum_{i,j=1}^{d_A} \sum_{m,r=1}^{d_B} \sum_{n,s=1}^{d_C} \langle i, m, n | \hat{\rho} | j, r, s \rangle | j, m, n \rangle \langle i, r, s |, \quad (24)$$

where  $d_X (X = A, B, C)$  refers to dimension of the Hilbert space of subsystem  $X$ . We use  $\hat{\rho}^{TA}$ ,  $\hat{\rho}^{TB}$ , and  $\hat{\rho}^{TC}$  to calculate the negativity measures for sub-systems  $A$ ,  $B$ , and  $C$ , respectively

For a quantum state  $\hat{\rho}$  in  $d$  dimensional Hilbert space, the linear entropy  $S_l$  is defined as

$$S_l = \frac{d}{d-1} (1 - \text{Tr}(\hat{\rho}^2)). \quad (25)$$

Linear entropy is used to measure the mixedness of subsystems  $A, B$ , and  $C$ . For pure states  $S_l = 0$ , whereas for maximally mixed states  $S_l = 1$ . Reduced state operators  $\hat{\rho}_{red}^A = \text{tr}_{BC}(\hat{\rho}_{ABC})$ ,  $\hat{\rho}_{red}^B = \text{tr}_{AC}(\hat{\rho}_{ABC})$ , and  $\hat{\rho}_{red}^C = \text{tr}_{AB}(\hat{\rho}_{ABC})$  are used to calculate linear entropy  $S_l$ , for the subsystems  $A, B$ , and  $C$ , respectively. Negativities and linear entropies are used to characterize the state of the composite system at an instant  $t$ , for a given value of coupling to the environment.

## NUMERICAL RESULTS AND CONCLUSIONS

We consider the system prepared in the state  $\hat{\rho}_S(0) = |g, 0, 0\rangle \langle g, 0, 0|$ , at  $t = 0$ . The laser-ion coupling constant is taken to be  $\Omega = 8.95 \text{ MHz}$  [5], where as the ratio  $\mu_{11}/a_{11} = 4.0$ . Numerical values of  $\Gamma(t)$  and  $C(t)$  are obtained by solving the integrals of Eqs. (17,18) for the choice  $\omega_c = 1200 \text{ MHz}$ , temperature  $T = 0.03 \text{ K}$  and different values of coupling strength  $\kappa$ . The variable  $\omega$  in Eqs. (17,18) is varied from zero to  $3\omega_c$ . The value  $\kappa = 0.001$  corresponds to a weak coupling and successively larger values tend to produce decoherence on a scale comparable to GHZ state generation time which is of the order of  $0.34 \text{ nano s}$ . The state of the system at an instant  $t$  can be detected experimentally by cavity-photon measurement combined with atomic population inversion measurement.

Figs. (1) and (2) display  $P_{GHZ}(t)$  and population inversion  $I(t)$ , respectively, as a function of scaled time variable  $T(= a_{11}t)$  for decoherence parameter values of  $\kappa = 0, 0.001, 0.01$ , and  $0.1$ . Evidently the evolution dynamics of

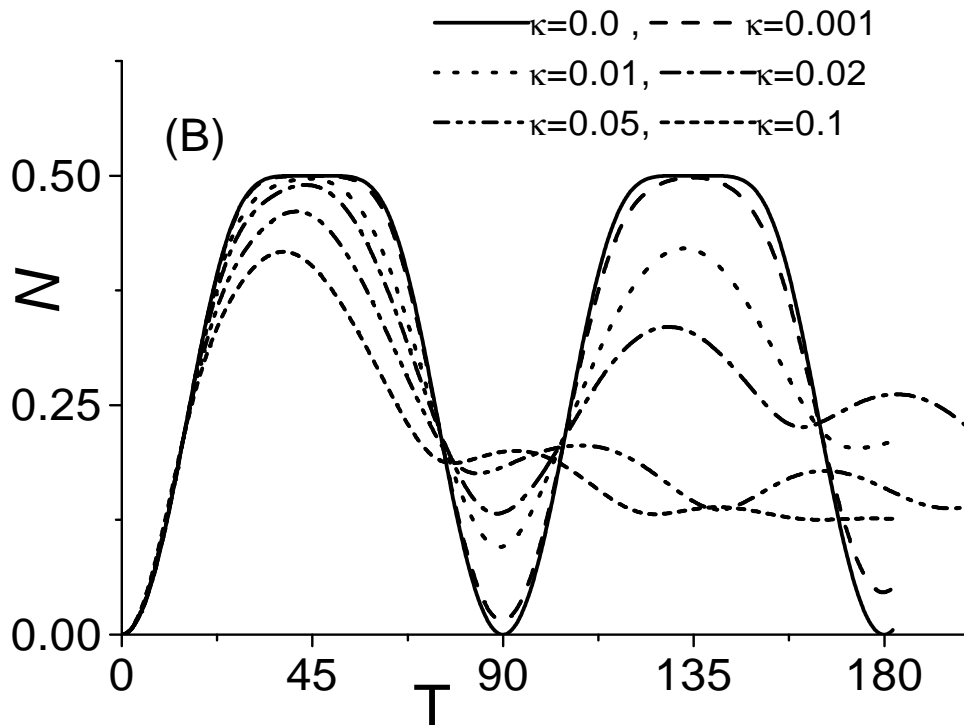


FIG. 4:  $N$ , calculated from  $\hat{\rho}^{TB} = \hat{\rho}^{TC}$ , as a function of scaled time variable  $T(= a_{11}t)$ , for the choice  $\mu_{11} \setminus a_{11} = 4$ , and  $\kappa = 0, 0.001, 0.01, 0.02, 0.05$  and  $0.1$ .

$P_{GHZ}(t)$  and  $I(t)$  is sensitive to changes in the decoherence parameter  $\kappa$ . The presence of decay factors in Eq. (20) causes the peak value of  $P_{GHZ}$  to decrease with time. Phase decoherence causes a shift in the interaction time needed to get the system in maximally entangled state. The population inversion however does not show any phase decoherence effects. We may point out that at  $T = 135^\circ$  the tripartite system is in maximally entangled state of Eq. (9) which is orthogonal to the state of Eq. (8) for which  $P_{GHZ}(t)$  has been calculated. Population inversion is zero at  $T = 45^\circ$  as well as  $135^\circ$ , signalling maximally entangled state generation. For weak coupling ( $\kappa = 0.001$ ), the behavior of  $I(t)$  does not differ much from no decoherence curve. However, for larger values of  $\kappa$ ,  $I(t)$  for the separable system at  $T = 45^\circ$  can indicate the amount of decoherence present.

The state operator of Eq. (19) for  $m = 1, n = 1$  is used to calculate the density matrices transposed with respect to quantum systems A, B, and C. The negativities are calculated, numerically, from  $\hat{\rho}^{TA}$ ,  $\hat{\rho}^{TB}$ , and  $\hat{\rho}^{TC}$  and plotted as a function of scaled time variable  $T(= a_{11}t)$ . The negativity plot displaying entanglement dynamics of internal state of two-level ion (A) is shown in Fig. 3. For subsystem B, the negativity calculated from  $\hat{\rho}^{TB} = \hat{\rho}^{TC}$ , is displayed as a function  $T(= a_{11}t)$  in Fig. 4. The values of decoherence parameter are  $\kappa = 0, 0.001, 0.01, 0.02, 0.05$  and  $0.1$ . The time evolution of vibrational motion of ion's center of mass(B) and cavity number state (C) are identical due to inherent symmetry of these subsystems. We notice that as the value of decoherence parameter increases, there is a decrease in the maximum entanglement of sub-systems A, B and C with their compliments. Besides that the phase decoherence changes the time at which maximal entanglement of the three parties is observed. These two factors are consistent with the behavior of  $P_{GHZ}(t)$  and  $I(t)$  in Figs. 1 and 2.

Linear entropies  $S_l$ , for subsystems A, B and C have been calculated using the reduced density operators obtained from  $\hat{\rho}_{IS}(t)$  of Eq. (19) for  $m = 1, n = 1$ . Figs. 5 and 6, display  $S_l$  as a function of scaled time variable  $T(= a_{11}t)$ , for subsystems A and B(or C), respectively. The decoherence parameter values are  $\kappa = 0, 0.001, 0.01, 0.02, 0.05$  and  $0.1$ . For  $\kappa = 0.001, 0.01$ , the trend of time evolution of linear entropy follows the variation of entanglement as seen in negativity plots of Figs. 3 and 4. However, for a stronger coupling value of  $\kappa = 0.02$  for subsystem A, whereas  $N$  tends to zero for  $T$  approaching  $90^\circ$ ,  $S_l$  shows fluctuation for  $T > 90^\circ$ . Similarly for  $\kappa = 0.05$  negativity indicates a decoupling of system A from system BC beyond  $T = 67^\circ$  while  $S_l$  points to the presence of some correlations. For  $\kappa = 0.1$ , the system is highly damped and both  $N$  and  $S_l$  show the ion to become separable around  $T = 45^\circ$ . We may conclude that for the states lying at the boundary of entangled separable region the negativity and linear entropy show distinctly different variation with time the reason being that the negativity measures only entanglement generating quantum correlations, whereas the linear entropy measures all correlations that reduce the purity of the

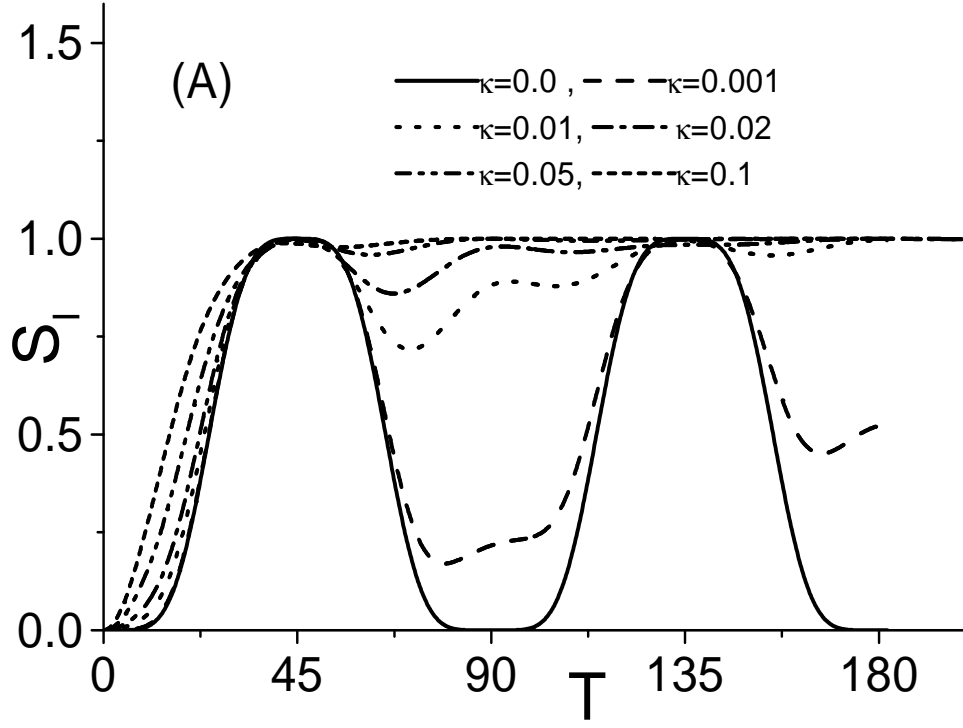


FIG. 5: Linear entropy  $S_l^A$ , calculated from  $\hat{\rho}_{red}^A$ , as a function of scaled time variable  $T(= a_{11}t)$ , for the choice  $\mu_{11} \setminus a_{11} = 4$ , and  $\kappa = 0, 0.001, 0.01, 0.02, 0.05$  and  $0.1$ .

state.

To conclude, we have investigated the decoherence process of three qubit system obtained by manipulating the state of a cold trapped two-level ion coupled to an optical cavity. Interaction of the ion with a resonant laser field and the cavity field tuned to red sideband of ionic vibrational motion, generates entanglement of internal states of the ion, vibrational states of ionic center of mass and the cavity field state. Non-dissipative decoherence of the state of the system occurs due to interaction of the system with the environment. We have considered the effect of decoherence sources such as magnetic field fluctuations, laser frequency fluctuations, potentials applied to electrodes and coupling to states outside the model space. The random perturbations of the Hamiltonian are accounted for by coupling the model space interaction Hamiltonian to the environment, modeled as a set of non-interacting harmonic oscillators. The pointer observable is energy of the isolated quantum system. Analytic expression for the state operator of tripartite composite system, including non dissipative decoherence effects has been obtained. The initial state of the tripartite system is a separable state and the state of environment has no initial correlations. Coupling to environment is found to introduce an exponential decay with time of the off diagonal matrix elements of density operator  $\hat{\rho}_{IS}(t)$ . In addition, a defasing of various states in the superposition also occurs. The extent to which the process is decohered depends on the system environment coupling strength, that can be partially controlled by adjusting the electrode potentials. Besides the strength of coupling to the environment, the energy spectrum of system Hamiltonian plays an important role in determining the decoherence rate of a given initial state of the composite system. For a specific choice of interaction parameters, the isolated system evolves to tripartite GHZ state [8]. We have evaluated analytically the probability of generating maximally entangled GHZ state, and the population inversion in the presence of non-dissipative decoherence. Numerical calculations for different values of system environment coupling strengths using interaction parameter from a recent experiment show the peak value of GHZ state generation probability to decrease with increase in  $\kappa$ .  $P_{GHZ}(t)$  is also sensitive to phase decoherence. The population inversion however does not show any phase decoherence effects. The results can be used to study the effects of engineered environment on the process of tripartite maximally entangled state generation. Bipartite entanglement of cavity mode and atomic internal states can be produced without coupling to the motional states. The tripartite entanglement generated through coupling to motional states can be transferred to other ions that might be added to the trap. In comparison with an earlier proposal for GHZ state generation [13], in the current scheme the initial state of the system is  $|g, 0, 0\rangle$ . As such the cavity losses and spontaneous decay effects are minimized.

Using negativity as an entanglement measure, the entanglement dynamics of the tripartite system in the presence

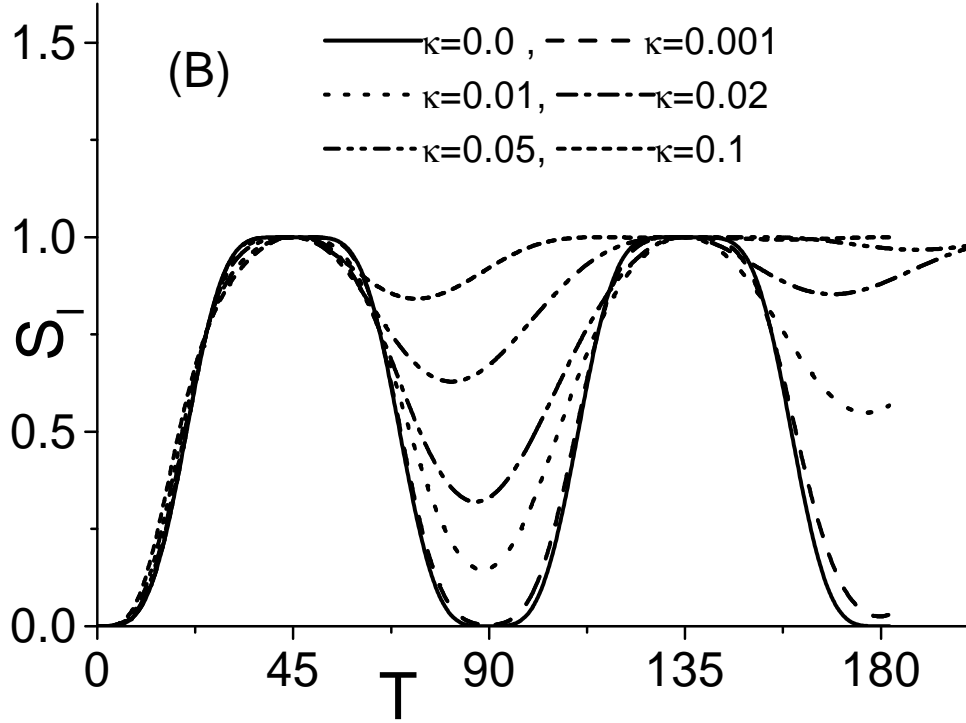


FIG. 6: Linear entropy  $S_l$ , calculated from  $\hat{\rho}_{red}^B$ , as a function of scaled time variable  $T(= a_{11}t)$ , for the choice  $\mu_{11} \setminus a_{11} = 4$ , and  $\kappa = 0, 0.001, 0.01, 0.02, 0.05$  and  $0.1$ .

of decoherence has been analyzed. As the value of decoherence parameter increases, the maximum entanglement of sub-systems  $A$  and  $B$  with their compliments decreases. In the context of trapped ion radiated by the single mode cavity field and an external resonant laser, the time for which the two level ion remains coupled to the state of vibrational motion and the cavity state decreases with increase in  $\kappa$ . For large values of  $\kappa$  the states of the composite system lying at the boundary of entangled-separable region are reached. For these states the negativity and linear entropy show distinctly different variation with time. This can be understood by noting that whereas the negativity measures entanglement generating quantum correlations, the linear entropy measures all correlations that reduce the purity of the state.

### Acknowledgments

S. S. Sharma and N. K. Sharma acknowledge financial support from CNPq, Brazil. E. de Almeida thanks Capes, Brazil for financial support.

---

\* shelly@uel.br

† eduardo@uel.br;

‡ nsharma@uel.br;

- [1] A. K. Ekert, Phys. Rev. Lett. **67**, 661 (1991).
- [2] C. H. Bennet and S. J. Wiesner, Phys. Rev. Lett. **69**, 2881 (1992).
- [3] C. H. Bennet, G. Brassard, C. Crépeau, R. Jozsa, A. Peres, and W. K. Wothers, Phys. Rev. Lett. **70**, 1895 (1993).
- [4] D.J. Wineland, C. Monroe, W.M Itano, D. Leibfried, B.E. King, and D.M. Meekhof, NIST J. Res. **103**, 259 (1998); Ch. Roos, Th. Zeiger, H. Rohde, H. C. Nagerl, J. Eschner, D. Liebfried, F. Schmidt-Kaler, R. Blatt, Phys.Rev. Lett. **83**, 4713 (1999).
- [5] A. B. Mundt, A. Kreuter, C. Russo, C. Becher, D. Leibfried, J. Eschner, F. Schmidt-Kaler, R. Blatt, Appl. Phys. B**76**, 117 (2003).
- [6] T. Pellizzari, J. I. Cirac, S. A. Gardiner, and P. Zoller, Phys. Rev. Lett. **75**, 3788 (1995).
- [7] J. I. Cirac, P. Zoller, H. J. Kimble, and H. Mabuchi, Phys. Rev. Lett. **78**, 3221 (1997).
- [8] S. Shelly Sharma, Phys. Letts. A **311**, 111 (2003).

- [9] F. Schmidt-Kaler, S. Gulde, M. Riebe, T. Deuschle, A. Kreuter, G. Lancaster, C. Becher, J. Eschner, H. Hffner, and R. Blatt, *J. Phys. B: At. Mol. Opt. Phys.* **36**, 623 (2003).
- [10] C. J. Myatt, B. E. King, Q. A. Turchette, C. A. Sackett, D. Kielpinski, W. M. Itano, C. Monroe, and D. J. Wineland, *Nature*, 403, 269 (2000).
- [11] Q. A. Turchette, C. J. Myatt, B. E. King, C. A. Sackett, D. Kielpinski, W. M. Itano, and D. J. Wineland, *Phys. Rev. A* **62**, 053807 (2000).
- [12] A. O. Caldeira, and A. J. Legget, *Physica A* **121**, 587 (1983).
- [13] C. Di Fidio, S. Maniscalco, and W. Vogel, *Phys. Rev. A*, **65**, 033825 (2002).
- [14] D. Mozyrsky and V. Privman, *J. Stat. Phys.* **91**, 787 (1998).
- [15] A. Peres, *Phys. Rev. Lett.* **77**, 1413 (1996); M. Horodecki, P. Horodecki, and R. Horodecki, *Phys. Lett. A* **223**, 1 (1996).
- [16] G. Vidal and R.F Werner, *Phys. Rev. A* **65**, 032314 (2002).
- [17] Q. A. Turchette, D. Kielpinski, B. E. King, D. Liebfried, D. M. Meekhof, C. J. Myatt, M. A. Rowe, C. A. Sackett, C. S. Wood, W. M. Itano, C. Monroe, and D. J. Wineland, *Phys. Rev. A* **61**, 063418 (2000).